Journal of Neurochemistry
Lippincott Williams & Wilkins, Inc., Philadelphia

Alzheimer's Presenilin-1 Mutation Potentiates Inositol 1,4,5-Trisphosphate-Mediated Calcium Signaling in *Xenopus* Oocytes

*‡Malcolm A. Leissring, †Brooke A. Paul, †Ian Parker, §Carl W. Cotman, and *‡Frank M. LaFerla

*Laboratories of *Molecular Neuropathogenesis and †Cellular and Molecular Neurobiology, and ‡Center for the Neurobiology of Learning and Memory, and §Institute for Brain Aging and Dementia: Department of Psychobiology, University of California at Irvine, Irvine, California, U.S.A.*

Abstract: Perturbations in intracellular Ca^{2+} signaling may represent one mechanism underlying Alzheimer's disease (AD). The presenilin-1 gene (*PS1*), associated with the majority of early onset familial AD cases, has been implicated in this signaling pathway. Here we used the *Xenopus* oocyte expression system to investigate in greater detail the role of PS1 in intracellular Ca^{2+} signaling pathways. Treatment of cells expressing wild-type PS1 with a cell surface receptor agonist to stimulate the phosphoinositide second messenger pathway evoked Ca^{2+}-activated Cl^- currents that were significantly potentiated relative to controls. To determine which elements of the signal transduction pathway are responsible for the potentiation, we used photolysis of caged inositol 1,4,5-trisphosphate (IP_3) and fluorescent Ca^{2+} imaging to demonstrate that PS1 potentiates IP_3-mediated release of Ca^{2+} from internal stores. We show that an AD-linked mutation produces a potentiation in Ca^{2+} signaling that is significantly greater than that observed for wild-type PS1 and that cannot be attributed to differences in protein expression levels. Our findings support a role for PS1 in modulating IP_3-mediated Ca^{2+} liberation and suggest that one pathophysiological mechanism by which *PS1* mutations contribute to AD neurodegeneration may involve perturbations of this function. **Key Words:** Alzheimer's disease—Presenilin—Calcium signaling—Inositol 1,4,5-trisphosphate.
J. Neurochem. **72,** 1061–1068 (1999).

Mutations in the presenilin-1 gene (*PS1*), located on chromosome 14, are linked to early onset, autosomal dominant Alzheimer's disease (AD) (Sherrington et al., 1995). The mechanisms by which these mutations subvert normal cellular functions, culminating in AD neurodegeneration, are not known. Converging evidence from studies involving cells isolated from carriers harboring PS1 mutations and transgenic models points to a role in increasing β-amyloid (Aβ) production (Duff et al., 1996; Scheuner et al., 1996; Citron et al., 1997). Although the molecular pathway(s) underlying this process is currently unresolved, one potential mechanism may involve alteration of intracellular Ca^{2+} signaling. Increasing Ca^{2+} levels in cultured cells have been shown to modulate the processing of the amyloid precursor protein, resulting in increased Aβ production (Querfurth and Selkoe, 1994), which suggests that perturbations in Ca^{2+} regulation may lie upstream of Aβ production.

Other roles for PS1 include a potential role in cellular signaling mechanisms, based on studies showing homology of PS1 to the *Caenorhabditis elegans* protein Sel-12, which facilitates signal transduction through the Notch/lin-12 family of receptors (Levitan and Greenwald, 1995). As PS1 is capable of rescuing egg-laying deficits in Sel-12-deficient worms (Levitan et al., 1996; Baumeister et al., 1997), this suggests that it too may play a similar role in modulating cell-signaling pathways. The topology of PS1, an integral membrane protein, has been proposed to consist of six to eight membrane-spanning domains (Doan et al., 1996; Li and Greenwald, 1996; Lehmann et al., 1997), causing some to suggest that PS1 may be involved in ion transport or as part of an ion channel (Clark et al., 1995; Li and Greenwald, 1996). The expression profile and localization of PS1 within the cell are also consistent with a potential role in regulating neuronal Ca^{2+} signaling. The *PS1* gene is ubiquitously expressed (Sherrington et al., 1995), but within the brain, neurons are the predominant expressing cell type (Cribbs et al., 1996; Kovacs et al., 1996). Within the cell, the PS1 molecule is localized predominantly to the endoplasmic reticulum (ER) (Ko-

Received September 4, 1998; revised manuscript received October 28, 1998; accepted October 28, 1998.

Address correspondence and reprint requests to Dr. F. M. LaFerla at Laboratory of Molecular Neuropathogenesis, Department of Psychobiology, University of California at Irvine, 1109 Gillespie Neuroscience Facility, Irvine, CA 92697-4545, U.S.A.

M. A. Leissring and B. A. Paul contributed equally to this study.

Abbreviations used: Aβ, β-amyloid; AD, Alzheimer's disease; ER, endoplasmic reticulum; c-IP_3, caged inositol 1,4,5-trisphosphate; IP_3, inositol 1,4,5-trisphosphate; LPA, lysophosphatidic acid; PS1, presenilin-1.

vacs et al., 1996), an organelle involved in Ca^{2+} sequestration and release (Berridge, 1998).

Direct evidence that mutations in PS1 perturb cellular Ca^{2+} signaling comes from several lines of study. Even prior to the isolation of the *PS1* gene itself, it was shown that fibroblasts isolated from chromosome 14-linked familial AD patients displayed alterations in Ca^{2+} signaling (McCoy et al., 1993; Ito et al., 1994). Subsequently, fibroblasts from other carriers of *PS1* mutations were also shown to have increased levels of acylphosphatase, an enzyme involved in regulating the ER Ca^{2+}-ATPase (Liguri et al., 1996). The most direct evidence that PS1 is involved in Ca^{2+} signaling is derived from studies by Guo et al. (1996, 1997), who have shown that Ca^{2+} homeostasis is perturbed in cultured PC12 cells expressing PS1 mutations.

To better define the elements of the intracellular pathway by which PS1 affects Ca^{2+} signaling, we studied the effects of both wild-type PS1 ($PS1_{WT}$) and an AD-linked mutation ($PS1_{M146V}$) in *Xenopus laevis* oocytes. Two unique features of these cells make them particularly well suited for the study of intracellular Ca^{2+} signaling. First, because *Xenopus* oocytes contain a plasma membrane Cl^- channel whose activation is sensitive to intracellular Ca^{2+} concentrations ($[Ca^{2+}]_i$), Ca^{2+} responses can be measured by recording evoked Ca^{2+}-activated Cl^- currents under voltage-clamped conditions (Miledi and Parker, 1984). Second, in this system, intracellular Ca^{2+} release is activated exclusively by inositol 1,4,5-trisphosphate (IP_3), as these cells do not express the ryanodine receptors that also mediate intracellular Ca^{2+} release in many other cell types.

Here we report that $PS1_{WT}$ potentiates Ca^{2+}-activated Cl^- currents evoked by lysophosphatidic acid (LPA), a cell surface agonist that activates the IP_3-linked signaling pathway (Tigyi et al., 1990). Using photolysis of caged IP_3 {c-IP_3; D-*myo*-inositol 1,4,5-trisphosphate, $P^{4(5)}$-[1-(2-nitrophenyl)ethyl ester]; Calbiochem, La Jolla, CA, U.S.A.} and fluorescent Ca^{2+} imaging, we show that this effect involves the potentiation of IP_3-mediated Ca^{2+} release. Moreover, the magnitude of the potentiation is significantly increased in cells expressing $PS1_{M146V}$ relative to $PS1_{WT}$-expressing cells, despite the fact that protein expression levels are similar for both conditions. Collectively, our findings indicate that PS1 modulates the IP_3-mediated release of Ca^{2+} and suggest that perturbations in this function caused by mutations in PS1 may contribute to the pathogenesis of early onset AD.

EXPERIMENTAL PROCEDURES

Mutagenesis and in vitro transcription

The $PS1_{M146V}$ missense mutation was introduced into human $PS1_{WT}$ cDNA contained in pGem plasmid (Cribbs et al., 1996), using the QuikChange Site-Directed Mutagenesis Kit (Stratagene, La Jolla, CA, U.S.A.) according to manufacturer's recommendations with the following two mutagenic oligonucleotides: 5′-ACCAGGAGGATAGTCACGACAACAATGACACTGAT-3′ and 5′-ATCAGTGTCATTGTTGTCGTGACTATCCTCCTGGT-3′. Both the mutant and the wild-type sequences were confirmed by DNA sequencing of the entire coding region.

In vitro RNA synthesis was performed by runoff transcription of linearized *PS1* cDNAs using the Riboprobe Gemini System (Promega, Madison, WI, U.S.A.) according to manufacturer's instructions. Each template plasmid was linearized with the restriction endonucleases *Pst*I or *Sac*II and used to generate sense or antisense cRNA, respectively. As several of our experiments involved comparisons between $PS1_{WT}$ and $PS1_{M146V}$ cRNA-injected oocytes, we employed several measures to minimize variability in the quality and quantity of the cRNA constructs to be injected into the oocytes. To that end, $PS1_{WT}$ and $PS1_{M146V}$ cRNAs were generated in parallel from equal amounts of linearized cDNA, and the concentrations of the resulting transcripts were determined spectrophotometrically. Additionally, a portion of each transcription product was analyzed on a denaturing agarose gel and visualized by ethidium bromide fluorescence to verify that comparable levels of full-length transcripts were produced. Finally, cRNA concentrations were diluted to a final concentration of 500 ng/μl and stored in small aliquots at −80°C.

Preparation of oocytes and cRNA injection

Oocytes obtained from adult *X. laevis* frogs (Xenopus I, Ann Arbor, MI, U.S.A.) were defolliculated by two 1-h treatments with 0.5 mg/ml collagenase and incubated overnight in normal Ringer's solution (120 m*M* NaCl, 2 m*M* KCl, 1.8 m*M* $CaCl_2$, 5 m*M* HEPES, pH 7.4) at 16°C. For cRNA injections, a piston-driven Nanoject microinjection apparatus (Drummond Scientific Co., Broomall, PA, U.S.A.) was fitted with glass electrodes pulled to tip diameters of ~15–20 μm that had been baked at 200°C for 1–7 days to eliminate any residual RNases. Stage V and VI oocytes were injected with 46 nl of the appropriate cRNA (500 ng/μl) or RNase-free H_2O. Injection volumes were checked periodically for consistency using a dissecting microscope fitted with an eyepiece reticule. Following microinjection, cells were incubated in Ringer's solution at 16°C for 2–4 days before recording. Throughout the incubation period, the Ringer's solution was changed twice daily and the health of the cells was closely monitored under a dissecting microscope.

Loading of c-IP_3 and Ca^{2+} indicator

For electrophysiological studies, oocytes were injected with 4 pmol of c-IP_3 using a pressure microinjector (General Valve Corp., Fairfield, NJ, U.S.A.) fitted with a freshly pulled glass pipette. Careful precautions were taken to ensure that all cells received equal amounts of c-IP_3. Oocytes of similar diameter (~1.2 mm; volume ~1 μl) were selected to minimize variations in the final intracellular concentration of c-IP_3 (~4 μ*M*). Before and after loading of each oocyte, the diameter of the droplet expelled by pressure pulse with the tip in the air was measured with an eyepiece reticule at 50× magnification; if any variation was evident, previously injected cells were discarded. In addition, to guard against any systematic changes in injection volume or c-IP_3 concentration, oocytes from different conditions were loaded in a rotating schedule. After loading with c-IP_3, cells were allowed to incubate for 30–45 min prior to recording to allow diffusion of c-IP_3 through these large cells. For Ca^{2+} imaging experiments, oocytes received injections containing 4 pmol of c-IP_3 combined with 40 pmol of the fluorescent Ca^{2+} indicator Oregon Green-5N (Molecular Probes, Eugene, OR, U.S.A.), yielding final concentrations of ~4 and ~40 μ*M*, respectively.

Flash photolysis

Photolysis of c-IP_3 to liberate free intracellular IP_3 was achieved using flashes of UV light (360–400 nm) derived from a mercury arc lamp fitted with an electronic shutter, which illuminated a spot of ~100 μm in diameter. The amount of IP_3 liberated was controlled by manipulating the durations of each flash. To establish a suitable range of flash durations, the intensity of the UV light was first adjusted through a variable neutral-density filter, which was kept constant throughout each experiment. Because Ca^{2+}-activated Cl^- channels are most densely concentrated in the animal hemisphere (Machaca and Hartzell, 1998), electrophysiological experiments were done by stimulating the animal hemisphere of albino oocytes, which was identified by the presence of the translucent germinal vesicle, evident by transillumination. Imaging experiments utilized pigmented oocytes; therefore, the vegetal hemisphere near the equator was stimulated because this region contains the least pigmentation.

Electrophysiology

Oocytes were impaled by two microelectrodes (resistance ~1–5 MΩ) filled with 3 *M* KCl and voltage clamped at −60 mV using a GeneClamp 500 (Axon Instruments, Burlingame, CA, U.S.A.) as described (Sumikawa and Miledi, 1989). Currents were low-pass filtered at 100 Hz and stored on floppy disk by a digital oscilloscope for subsequent analysis. To generate agonist-evoked responses, cells were continuously superfused with Ringer's solution and subjected to 5-s pulses of 10 μM LPA (Sigma Chemical Co., St. Louis, MO, U.S.A.). All electrophysiological experiments were performed at 20°C. Statistical comparisons were made using two-factor ANOVA with replication. All results are presented as mean values ± SEM.

Fluorescent Ca^{2+} imaging

Ca^{2+} fluorescence changes in response to photoreleased IP_3 were imaged using an Odyssey video-rate laser-scanned confocal microscope (Noran Instruments, Middleton, WI, U.S.A.) interfaced to an Olympus IMT-2 inverted microscope (Olympus, Tokyo, Japan) (Yao et al., 1995). Video signals were recorded using a professional S-VHS recorder (Sony SVO-9500MD; Sony Corp., Tokyo, Japan). Image analysis was performed off-line using the Meta-Morph software package (Universal Imaging Corp., West Chester, PA, U.S.A.) running on an IBM-compatible PC equipped with a Matrox LC video card (Matrox Electronic Systems, Dorval, Montreal, Canada) (Yao et al., 1995; Parker et al., 1997). Fluorescence intensities were measured within representative ~25-μm^2 areas of the video image. Fluorescence intensities are expressed as the change in intensity over the basal level of fluorescence prior to stimulation ($\Delta F/F_0$).

Western blotting

Protein extracts were prepared from PS1-injected and control oocytes as described (Callamaras and Parker, 1994), and protein concentrations were determined by the Bradford method. Equal amounts of protein (10 μg) were incubated briefly at 37°C, separated by sodium dodecyl sulfate–polyacrylamide gel electrophoresis on a 12% acrylamide gel, transferred to a nitrocellulose membrane, and blocked overnight in SuperBlock (Pierce, Rockford, IL, U.S.A.). The blot was incubated with primary antibody in Tris-buffered saline (pH 7.5) supplemented with 0.2% Tween 20 for several hours at room temperature and processed essentially as described previously (Weber et al., 1996) using the Ultra enhanced chemiluminescence kit (Pierce). PS1 antibodies and dilutions used in this study include SW2 (1:500; Weber et al., 1996), N-terminal fragment- and C-terminal fragment-specific antibodies (1:200; Chemicon, Temecula, CA, U.S.A.), and $PS1_{NT}$ and $PS1_{\alpha loop}$ (1:5,000; Thinakaran et al., 1996, 1998). Densitometric quantification of immunoblots was conducted using the Stratagene Eagle Eye II gel documentation system according to manufacturer's recommendation (Stratagene).

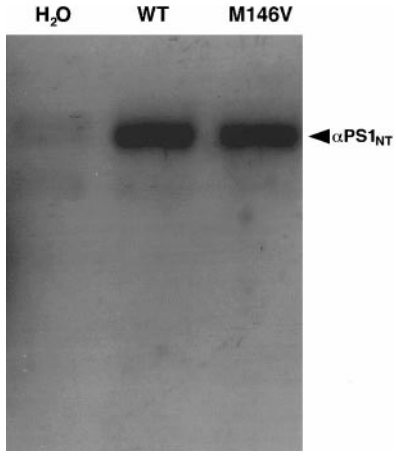

FIG. 1. Wild-type and mutant PS1 proteins accumulate to similar levels in *Xenopus* oocytes. Shown is representative protein blot of extracts prepared from oocytes that had been injected with H_2O, $PS1_{WT}$ cRNA, or $PS1_{M146V}$ cRNA. Antibody $PS1_{NT}$ (Thinakaran et al., 1998) was used to detect PS1 protein expression. Note that only the holoprotein is detected and that the levels of the wild-type and mutant proteins are comparable. Quantification of digitized images of immunoblots revealed that the $PS1_{WT}$ and $PS1_{M146V}$ proteins accumulated to levels within 5% of each other and that both were approximately three times greater than in control cells.

RESULTS

One advantage of the *Xenopus* oocyte system is that these cells readily express introduced foreign molecules. Accurate determination of protein expression levels was of central importance for the present study, as one of our goals was to determine whether evoked Ca^{2+} responses were different in cells expressing $PS1_{WT}$ and $PS1_{M146V}$. Some of the injected oocytes were randomly selected for protein expression analysis by western blot, whereas the remaining cells were used in the electrophysiological experiments described below. Figure 1 shows a representative western blot of protein extracts prepared from H_2O-, $PS1_{WT}$-, and $PS1_{M146V}$-injected oocytes stained with the $PS1_{NT}$ antibody (Thinakaran et al., 1998), revealing high levels of expression of both the wild-type and the mutant proteins relative to controls. Two points are worth noting. First, despite using an antibody that is capable of detecting the N-terminal proteolytic fragment of PS1 (Thinakaran et al., 1998) and despite our ability to detect this ~30-kDa fragment in mouse brain extracts (data not shown), we did not detect the proteolytic fragments of PS1 in the oocyte extracts. Rather, under our conditions, only the holoprotein was detected in the western blot, which was recognized by a wide variety of

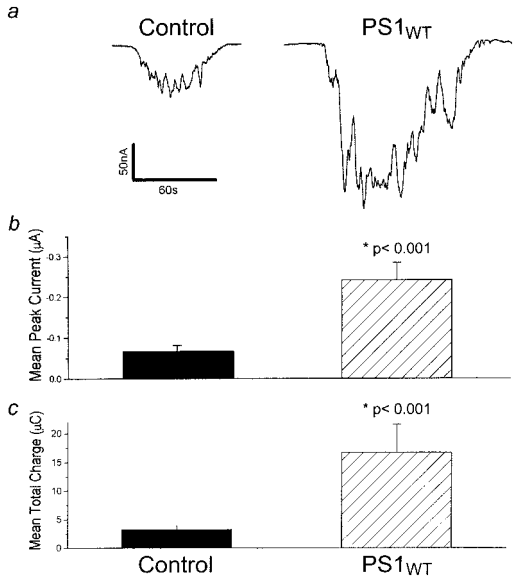

FIG. 2. Agonist-evoked Ca^{2+}-activated Cl^- currents are potentiated in cells overexpressing $PS1_{WT}$. **a:** Representative whole-cell Ca^{2+}-activated Cl^- currents from *Xenopus* oocytes previously injected with either $PS1_{WT}$ cRNA or H_2O measured with a two-electrode voltage clamp. LPA (10 μM) was bath applied for 5 s in each case. **b:** Mean peak currents evoked by LPA in $PS1_{WT}$-expressing oocytes (n = 13) and controls (n = 17). **c:** Mean total charge transferred per response (integral under current response). Data are from same experiments as in b.

antibodies, including those directed against the N- and C-terminal portions of PS1 (see Experimental Procedures for list of antibodies used). Second, and more importantly, the wild-type and mutant proteins accumulate to similar levels in the injected oocytes. Quantification of digital images of immunoblots revealed that protein levels did not differ by >5%, a result that was observed in several experiments (e.g., see legend to Fig. 1). Therefore, differences in electrophysiological responses between these two groups of cells are not likely attributable to quantitative differences in protein expression levels.

$PS1_{WT}$ potentiates LPA-evoked Ca^{2+}-activated Cl^- currents

To test whether expression of $PS1_{WT}$ modulates intracellular Ca^{2+} signaling in *Xenopus* oocytes, we recorded currents evoked by LPA (10 μM) in voltage-clamped cells injected 2–4 days previously with either sense or antisense $PS1_{WT}$ cRNA or H_2O. Compared with H_2O- and antisense-injected controls from the same donor frogs, oocytes injected with sense $PS1_{WT}$ cRNA produced significantly larger currents following application of LPA (Fig. 2a). LPA-evoked responses in antisense- and H_2O-injected cells were indistinguishable (data not shown); hence, only H_2O-injected oocytes were used as controls in subsequent experiments.

To facilitate statistical comparison of responses in $PS1_{WT}$-expressing oocytes and H_2O-injected controls, current traces were quantified according to mean peak current and total charge transferred. We found that the absolute magnitude of the LPA-evoked mean peak current in the H_2O-injected control cells averaged ~0.07 μA (Fig. 2b, filled column), whereas a significantly larger mean peak current of ~0.25 μA was observed in cells expressing $PS1_{WT}$ (Fig. 2b, hatched column; $p < 0.001$). Likewise, the mean total charge transferred in response to fixed (5-s) pulses of LPA, obtained by integrating the area under each current trace, was also significantly greater for $PS1_{WT}$-expressing cells relative to controls (~3 vs. ~17 μC, respectively; Fig. 2c; $p < 0.001$). Therefore, expression of $PS1_{WT}$ in *Xenopus* oocytes results in potentiation of agonist-evoked Ca^{2+}-activated Cl^- currents, suggesting that PS1 may play a role in modulating Ca^{2+} signaling.

Potentiation of Ca^{2+}-activated Cl^- currents by $PS1_{WT}$ occurs downstream of IP_3 production

Modulation of agonist-evoked currents by $PS1_{WT}$ could, in principle, be mediated by any of the numerous elements along the signal transduction cascade (e.g., cell surface receptors, G proteins, phospholipase C, IP_3 receptors, Ca^{2+}-activated Cl^- channels). To circumvent signaling elements upstream of IP_3 production, we directly manipulated intracellular IP_3 levels using c-IP_3, a chemically modified form of IP_3 that is nonmetabolizable and physiologically inert but is photolyzed by UV light to liberate free intracellular IP_3 (Callamaras and Parker, 1998). Hence, by changing the duration of UV light flashes, varying amounts of IP_3 can be liberated reproducibly in different oocytes.

H_2O-injected controls exhibited IP_3-evoked Cl^- currents that increased in size in response to increasing flash durations, eventually reaching an asymptotic maximum for flash durations ≥30 ms; no currents were evoked for flash durations ≤10 ms (Fig. 3b and d, circles). Compared with control cells, $PS1_{WT}$-expressing oocytes exhibited responses that were consistently larger for all flash durations tested and that reached an asymptotic maximum approximately twice as large as that seen in control cells (Fig. 3b and d, triangles). Statistical comparison of responses to flash durations ≥60 ms revealed that IP_3-evoked currents in cells expressing $PS1_{WT}$ were significantly greater than in controls in terms of both mean peak current ($p < 0.002$; Fig. 3c) and mean total charge transferred per response ($p < 0.001$; Fig. 3e). We also found that shorter flash durations were required to elicit a response in $PS1_{WT}$-expressing cells relative to controls, indicating that the threshold IP_3 level required to elicit a response was decreased by $PS1_{WT}$.

Potentiation of IP_3-evoked Ca^{2+} activated Cl^- currents is enhanced by AD-linked mutant $PS1_{M146V}$

Another important aim of these experiments was to determine if a mutant form of PS1 known to cause AD might yield IP_3-evoked responses that differ from those

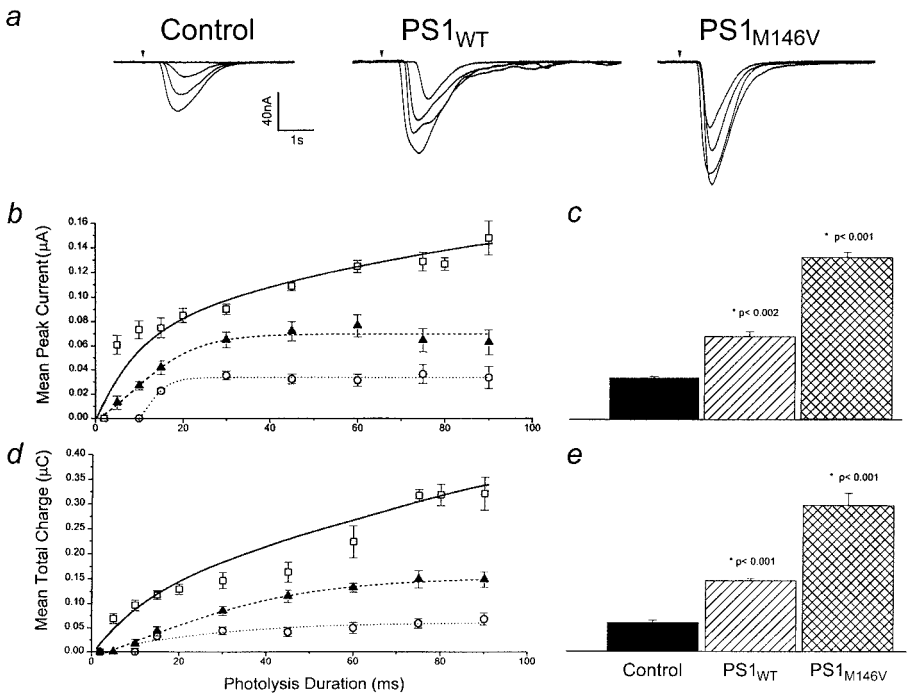

FIG. 3. IP_3-evoked Ca^{2+}-activated Cl^- currents are potentiated by wild-type PS1 and to a greater extent by mutant PS1. **a:** Representative families of Ca^{2+}-activated Cl^- currents evoked by photoreleased IP_3 in individual cells expressing $PS1_{WT}$ or $PS1_{M146V}$ and a control. Oocytes were injected with 4 pmol of c-IP_3 and stimulated by flashes of UV light applied to the animal hemisphere (arrowheads). Traces show responses to 10-, 15-, 30-, and 90-ms flash durations. **b:** Mean peak currents in control (circles), $PS1_{WT}$-expressing (triangles), and mutant $PS1_{M146V}$-expressing (squares) oocytes as a function of flash duration. Data points are mean ± SEM values from five to nine oocytes. **c:** Mean responses for flashes ≥60 ms. The *p* values apply to comparisons between $PS1_{WT}$ and control responses (middle column) and $PS1_{M146V}$ and $PS1_{WT}$ responses (right column). **d** and **e:** Similar analysis of measurements of total charge transferred during IP_3-evoked responses. Data are from same experiments as in b and c.

observed in cells expressing the wild-type protein. We chose to study the AD-linked *PS1* missense mutation that results in a methionine-to-valine substitution at amino acid 146, $PS1_{M146V}$, as this mutation causes an aggressive form of early onset AD (Van Broeckhoven, 1995) and has been shown to significantly increase the production of $A\beta_{1-42(43)}$ both in vitro and in vivo (Borchelt et al., 1996; Duff et al., 1996). Accordingly, $PS1_{WT}$- and $PS1_{M146V}$-expressing cells were compared to determine how IP_3-evoked currents were affected.

Like $PS1_{WT}$-expressing cells, oocytes expressing $PS1_{M146V}$ exhibited a significant potentiation in IP_3-evoked currents relative to controls. Strikingly, however, the magnitude of this potentiation was greatly increased in cells expressing $PS1_{M146V}$ compared with responses of $PS1_{WT}$-expressing cells for all flash durations tested (Fig. 3b and d, squares). Interestingly, unlike $PS1_{WT}$-expressing cells or controls, IP_3-evoked responses in $PS1_{M146V}$-expressing cells did not reach a clear asymptotic maximum within the range of flash durations tested, as assessed by either mean peak current (Fig. 3b) or total charge transferred per response (Fig. 3d). Nonetheless, statistical comparison of IP_3-evoked responses to flash durations ≥60 ms revealed that currents evoked in $PS1_{M146V}$-expressing cells were significantly potentiated relative to $PS1_{WT}$-expressing cells ($p < 0.001$; Fig. 3c and e). Threshold IP_3 levels (i.e., flash durations) were also decreased in $PS1_{M146V}$-expressing cells to an even greater extent than was observed in cells expressing $PS1_{WT}$, suggesting that additional sensitivity to IP_3 is conferred by $PS1_{M146V}$ (Fig. 3b and d).

Ca^{2+} imaging reveals that IP_3-mediated Ca^{2+} release is potentiated by $PS1_{WT}$ and to a greater extent by $PS1_{M146V}$

The potentiation in Cl^- currents induced by PS1 might be due to up-regulation of the Ca^{2+}-activated Cl^- channels themselves rather than to direct changes in IP_3-mediated Ca^{2+} release. This is of particular concern as, in other cell types, functional K^+ channels have been reported to be up-regulated by PS1 (Malin et al., 1998). To resolve this issue, we imaged changes in $[Ca^{2+}]_i$ by loading cells with the fluorescent Ca^{2+} indicator Oregon Green-5N and measuring changes in normalized fluorescence evoked by photorelease of IP_3 using laser-scanned confocal microscopy.

IP_3-evoked fluorescence signals were potentiated in cells expressing $PS1_{WT}$ and to a greater extent $PS1_{M146V}$-expressing cells relative to controls (Fig. 4a), consistent with the findings for Ca^{2+}-activated Cl^- currents. Mean peak fluorescence changes also showed lower thresholds for activation and reached higher asymptotic maxima in $PS1_{WT}$-expressing cells and to a greater extent in $PS1_{M146V}$-expressing cells relative to controls for a range of flash durations tested (Fig. 4b). Statistical comparison of responses to flash durations ≥500 ms revealed significant differences between $PS1_{WT}$-expressing cells and controls ($p < 0.001$, Fig. 4c) as well as between $PS1_{M146V}$- and $PS1_{WT}$-expressing cells ($p < 0.001$; Fig. 4c). These findings indicate that $PS1_{WT}$ and, to a greater extent, $PS1_{M146V}$ potentiate IP_3-mediated Ca^{2+} release.

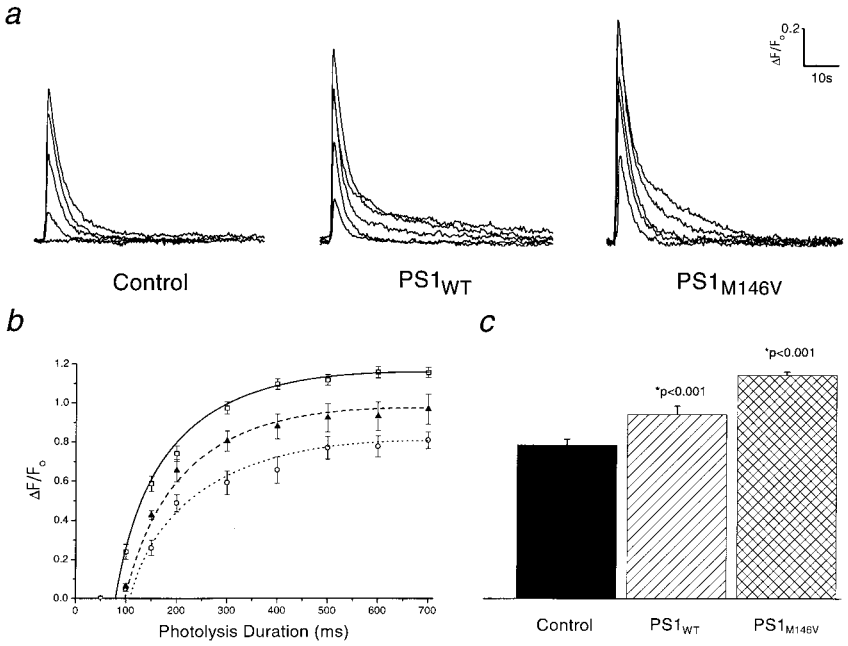

FIG. 4. Ca^{2+} imaging demonstrates that PS1 potentiates IP_3-mediated Ca^{2+} release. **a:** Representative families of recordings of changes in Ca^{2+} fluorescence intensity ($\Delta F/F_0$) evoked by photoreleased IP_3 in $PS1_{WT}$- and $PS1_{M146V}$-expressing cells and a control. Oocytes were injected with 4 pmol of c-IP_3 and 40 pmol of Oregon Green-5N and stimulated by flashes of UV light applied to the vegetal hemisphere near the equator. Traces show normalized fluorescence responses ($\Delta F/F_0$) to 100-, 150-, 200-, 400-, and 700-ms flash durations. **b:** Mean peak fluorescence intensity in control (circles), $PS1_{WT}$-expressing (triangles), and mutant $PS1_{M146V}$-expressing (squares) oocytes as a function of flash duration. Data points are mean ± SEM values from 8–11 oocytes. **c:** Mean responses for flashes ≥500 ms. The *p* values apply to comparisons between $PS1_{WT}$ and control responses (middle column) and $PS1_{M146V}$ and $PS1_{WT}$ responses (right column).

DISCUSSION

Perturbations in intracellular Ca^{2+} homeostasis have been documented in both familial and sporadic forms of AD (for reviews, see Khachaturian, 1994; Mattson et al., 1998). With the identification and isolation of genes causally linked to AD, it has become possible to investigate whether alterations in Ca^{2+} signaling represent a cause or a consequence of AD neuropathology. In this study, we examined the role of PS1 in modulating the IP_3/Ca^{2+} signaling cascade.

In initial experiments, we activated the phosphoinositide second messenger cascade with the cell surface receptor agonist LPA. Using Ca^{2+}-activated Cl^- currents as an endogenous measure of intracellular Ca^{2+} release, we found that overexpression of $PS1_{WT}$ resulted in a significant potentiation in LPA-evoked Cl^- currents. To further elucidate which elements in this complex signaling pathway are modulated by PS1, we used photolysis of c-IP_3 to circumvent the many upstream signaling elements. In addition, we used fluorescent Ca^{2+} imaging to rule out possible effects on the Cl^- channels themselves. Both strategies demonstrated that $PS1_{WT}$ potentiates Ca^{2+} signals by modulating the IP_3-mediated release of Ca^{2+}. Furthermore, the AD-linked mutation $PS1_{M146V}$ was tested and shown to potentiate IP_3-evoked Ca^{2+} signaling to a significantly greater extent than $PS1_{WT}$ due to mechanism(s) not attributable to differences in protein expression levels.

Our results add to a growing list of studies showing potentiated Ca^{2+} signaling in cells expressing missense mutations in PS1. In particular, bombesin-activated Ca^{2+} signals have been shown to be disturbed in fibroblasts isolated from a number of familial AD cases, including those containing the mutation $PS1_{A246Q}$ (McCoy et al., 1993; Ito et al., 1994). Similar disturbances have been reported in PC12 cells expressing $PS1_{L286V}$ (Guo et al., 1996). Hence, the potentiation in Ca^{2+} signaling we observe with $PS1_{M146V}$ does not appear to be specific to this mutation, but rather our findings lend support to the hypothesis that potentiation of Ca^{2+} signaling represents a general consequence shared by many PS1 mutations.

Although previous studies have documented perturbations in IP_3-linked Ca^{2+} signaling in several systems expressing PS1 mutations (Ito et al., 1994; Guo et al., 1996, 1997), any of several steps along this complex signal transduction pathway might have been responsible for the observed effects. Here, we provide direct evidence that the IP_3-mediated release of Ca^{2+} from internal stores is specifically modulated by PS1. Although the precise mechanism by which PS1 affects Ca^{2+} signaling remains to be elucidated, several clues are provided by the present study. First, in cells expressing either $PS1_{WT}$ or $PS1_{M146V}$, lower threshold amounts of IP_3 are required to elicit detectable Ca^{2+}-activated Cl^- currents and fluorescent Ca^{2+} changes. Second, the maximal levels of IP_3-evoked Ca^{2+} responses are also elevated in these cells. Both of these findings suggest an increased sensitivity to IP_3 that is more pronounced in cells expressing $PS1_{M146V}$ than $PS1_{WT}$.

Another point worth noting is that expression of PS1 in *Xenopus* oocytes leads to the production of the full-length protein. Although many reports show that PS1 is proteolytically processed to generate N- and C-terminal fragments of ~30 and ~20 kDa, respectively (Thinakaran et al., 1996), we do not detect any evidence of proteolytic fragments in our system, despite using numerous well-characterized antibodies specific for both fragments (Thinakaran et al., 1998). Although the lack of

processing in this system may reflect species differences and/or procedural artifacts (e.g., incubation at 16°C), our results are consistent with those of several studies showing that overexpression of exogenous PS1 leads preferentially to the accumulation of the full-length protein (Thinakaran et al., 1996; Baumann et al., 1997). Therefore, our results suggest that the holoprotein is responsible for the potentiation of IP_3-mediated Ca^{2+} release conferred by both $PS1_{WT}$ and $PS1_{M146V}$. Consistent with this interpretation, recent subcellular fractionation studies have shown that the holoprotein is predominantly localized to the ER, whereas the proteolytic fragments are localized to the Golgi compartment (Zhang et al., 1998), thus suggesting that the holoprotein is more likely to be involved in modulating ER functions such as Ca^{2+} signaling. Hence, even if the fragments do have some physiological role(s), the PS1 holoprotein appears to be the functional species involved in regulating Ca^{2+} signaling in our system.

Disturbances in the IP_3/Ca^{2+} signaling cascade could account for several hallmark features of AD, including increased vulnerability to neuronal cell death and deficits in learning and memory. Moreover, the finding that increasing $[Ca^{2+}]_i$ enhances Aβ production (Querfurth and Selkoe, 1994; Querfurth et al., 1995) suggests that changes in this Ca^{2+} signaling pathway might lie upstream in the events leading to AD neurodegeneration. Consequently, further research into the role of PS1 in this ubiquitous intracellular pathway should yield novel targets for therapeutic intervention.

Acknowledgment: We thank Dr. Charles Glabe for the SW2 antibody to PS1, Dr. Gopal Thinakaran for the $PS1_{NT}$ and $PS1_{\alpha loop}$ antibodies, Dr. Lian-sheng Chen for technical assistance, and Dr. Nicholas Callamaras for extensive procedural assistance and critical reading of the manuscript. This study was supported by the UCI–Markey Program in Human Neurobiology, grants from NIA (no. 13007) and NIGMS (no. 48071), and a scholarship from the Glenn Foundation/American Federation of Aging Research awarded to M.A.L.

REFERENCES

Baumann K., Paganetti P. A., Sturchler-Pierrat C., Wong C., Hartmann H., Cescato R., Frey P., Yankner B. A., Sommer B., and Staufenbiel M. (1997) Distinct processing of endogenous and overexpressed recombinant presenilin 1. *Neurobiol. Aging* **18,** 181–189.

Baumeister R., Leimer U., Zweckbronner I., Jakubek C., Grunberg J., and Haass C. (1997) Human presenilin-1, but not familial Alzheimer's disease (FAD) mutants, facilitate *Caenorhabditis elegans* Notch signalling independently of proteolytic processing. *Genes Funct.* **1,** 149–159.

Berridge M. J. (1998) Neuronal calcium signaling. *Neuron* **21,** 13–26.

Borchelt D. R., Thinakaran G., Eckman C. B., Lee M. K., Davenport F., Ratovitsky T., Prada C. M., Kim G., Seekins S., Yager D., Slunt H. H., Wang R., Seeger M., Levey A. I., Gandy S. E., Copeland N. G., Jenkins N. A., Price D. L., Younkin S. G., and Sisodia S. S. (1996) Familial Alzheimer's disease-linked presenilin 1 variants elevate Abeta1-42/1-40 ratio in vitro and in vivo. *Neuron* **17,** 1005–1013.

Callamaras N. and Parker I. (1994) Inositol 1,4,5-trisphosphate receptors in *Xenopus laevis* oocytes: localization and modulation by Ca^{2+}. *Cell Calcium* **15,** 66–78.

Callamaras N. and Parker I. (1998) Caged inositol 1,4,5-trisphosphate for studying release of Ca^{2+} from intracellular stores. *Methods Enzymol.* **291,** 380–403.

Citron M., Westaway D., Xia W., Carlson G., Diehl T., Levesque G., Johnson-Wood K., Lee M., Seubert P., Davis A., Kholodenko D., Motter R., Sherrington R., Perry B., Yao H., Strome R., Lieberburg I., Rommens J., Kim S., Schenk D., Fraser P., St. George-Hyslop P. H., and Selkoe D. J. (1997) Mutant presenilins of Alzheimer's disease increase production of 42-residue amyloid β-protein in both transfected cells and transgenic mice. *Nat. Med.* **3,** 67–72.

Clark R. F., Hutton M., Fuldne R. A., Froelich S., Karran E., Talbot C., Crook R., Lendon C., Prihar G., He C., Korenblat K., Martinez A., Wragg M., Busfield F., Behrens M. I., Myers A., Norton J., Morris J., Mehta N., Pearson C., Lincoln S., Baker M., Duff K., Zehr C., Perez-Tur J., Houlden H., Ruiz A., Ossa J., Lopera F., Arcos M., Madrigal L., Collinge J., Humphreys C., Ashworth A., Sarner S., Fox N., Harvey R., Kennedy A., Roques P., Cline R. T., Philips C. A., Venter J. C., Forsell L., Axelman K., Lilius L., Johnston J., Cowburn R., Viitanen M., Winblad B., Kosik K., Haltia M., Poyhonen M., Dickson D., Mann D., Neary D., Snowden J., Lantos P., Lannfelt L., Rossor M., Roberts G. W., Adams M. D., Hardy J., and Goate A. (1995) The structure of the presenilin 1 (S182) gene and identification of six novel mutations in early onset AD families. Alzheimer's Disease Collaborative Group. *Nat. Genet.* **11,** 219–222.

Cribbs D. H., Chen L.-S., Bende S. M., and LaFerla F. M. (1996) Widespread neuronal expression of the presenilin-1 early-onset Alzheimer's disease gene in the murine brain. *Am. J. Pathol.* **148,** 1797–1806.

Doan A., Thinakaran G., Borchelt D. R., Slunt H. H., Ratovitsky T., Podlisny M., Selkoe D. J., Seeger M., Gandy S. E., Price D. L., and Sisodia S. S. (1996) Protein topology of presenilin 1. *Neuron* **17,** 1023–1030.

Duff K., Eckman C., Zehr C., Yu X., Prada C.-M., Perez-tur J., Hutton M., Buee L., Harigaya Y., Yager D., Morgan D., Gordon M. N., Holcomb L., Refolo L., Zenk B., Hardy J., and Younkin S. (1996) Increased amyloid-β42(43) in brains of mice expressing mutant presenilin 1. *Nature* **383,** 710–713.

Guo Q., Furukawa K., Sopher B. L., Pham D. G., Martin G. M., and Mattson M. P. (1996) Alzheimer's PS-1 mutation perturbs calcium homeostasis and sensitizes PC12 cells to death induced by amyloid β-peptide. *Neuroreport* **8,** 379–383.

Guo Q., Sopher B. L., Furukawa K., Pham D. G., Robinson N., Martin G. M., and Mattson M. P. (1997) Alzheimer's presenilin mutation sensitizes neural cells to apoptosis induced by trophic factor withdrawal and amyloid β-peptide: involvement of calcium and oxyradicals. *J. Neurosci.* **17,** 4212–4222.

Ito E., Oka K., Etcheberrigaray R., Nelson T. J., McPhie D. L., Tofel-Grehl B., Gibson G. E., and Alkon D. L. (1994) Internal Ca^{2+} mobilization is altered in fibroblasts from patients with Alzheimer's disease. *Proc. Natl. Acad. Sci. USA* **91,** 534–538.

Khachaturian Z. S. (1994) Calcium hypothesis of Alzheimer's disease and brain aging. *Ann. NY Acad. Sci.* **747,** 1–11.

Kovacs D. M., Fausett H. J., Page K. J., Kim T. W., Moir R. D., Merriam D. E., Hollister R. D., Hallmark O. G., Mancini R., Felsenstein K. M., Hyman B. T., Tanzi R. E., and Wasco W. (1996) Alzheimer-associated presenilins 1 and 2: neuronal expression in brain and localization to intracellular membranes in mammalian cells. *Nat. Med.* **2,** 224–229.

Lehmann S., Cheisa R., and Harris D. A. (1997) Evidence for a six-transmembrane domain structure of presenilin 1. *J. Biol. Chem.* **272,** 12047–12051.

Levitan D. and Greenwald I. (1995) Facilitation of lin-12-mediated signalling by sel-12, a *Caenorhabditis elegans* S182 Alzheimer's disease gene. *Nature* **377,** 351–354.

Levitan D., Doyle T. G., Brousseau D., Lee M. K., Thinakaran G., Slunt H. H., Sisodia S. S., and Greenwald I. (1996) Assessment of normal and mutant human presenilin function in *Caenorhabditis elegans. Proc. Natl. Acad. Sci. USA* **93,** 14940–14944.

Li X. and Greenwald I. (1996) Membrane topology of the *C. elegans* sel-12 presenilin. *Neuron* **17,** 1015–1021.

Liguri G., Cecchi C., Latorraca S., Pieri A., Sorbi S., Degl'Innocenti D., and Ramponi G. (1996) Alteration of acylphosphatase levels in familial Alzheimer's disease fibroblasts with presenilin gene mutations. *Neurosci. Lett.* **210,** 153–156.

Machaca K. and Hartzell H. C. (1998) Asymmetrical distribution of Ca-activated Cl channels in *Xenopus* oocytes. *Biophys. J.* **74,** 1286–1295 [erratum in *Biophys. J.* (1998) **74,** 3313].

Malin S. A., Guo W.-X. A., Jafari G., Goate A. M., and Nerbonne J. M. (1998) Presenilins upregulate functional K^+ channel currents in mammalian cells. *Neurobiol. Dis.* **4,** 398–409.

Mattson M. P., Guo Q., Furukawa K., and Pedersen W. A. (1998) Presenilins, the endoplasmic reticulum, and neuronal apoptosis in Alzheimer's disease. *J. Neurochem.* **70,** 1–14.

McCoy K. R., Mullins R. D., Newcomb T. G., Ng G. M., Pavlinkova G., Polinsky R. J., Nee L. E., and Sisken J. E. (1993) Serum- and bradykinin-induced calcium transients in familial Alzheimer's fibroblasts. *Neurobiol. Aging* **14,** 447–455.

Miledi R. and Parker I. (1984) Chloride current induced by injection of calcium into *Xenopus* oocytes. *J. Physiol. (Lond.)* **357,** 173–183.

Parker I., Callamaras N., and Wier W. G. (1997) A high-resolution, confocal laser-scanning microscope and flash photolysis system for physiological studies. *Cell Calcium* **21,** 441–452.

Querfurth H. W. and Selkoe D. J. (1994) Calcium ionophore increases amyloid β-peptide production by cultured cells. *Biochemistry* **33,** 4550–4561.

Querfurth H. W., Wijsman E. M., St. George-Hyslop P. H., and Selkoe D. J. (1995) Beta APP mRNA transcription is increased in cultured fibroblasts from the familial Alzheimer's disease-1 family. *Brain Res. Mol. Brain Res.* **28,** 319–337.

Scheuner D., Eckman C., Jensen M., Song X., Citron M., Suzuki N., Bird T. D., Hardy J., Hutton M., Kukull W., Larson E., Levy-Lahad E., Viitanen M., Peskind E., Poorkaj P., Schellenberg G., Tanzi R., Wasco W., Lannfelt L., Selkoe D., and Younkin S. (1996) Secreted amyloid β-protein similar to that in the senile plaques of Alzheimer's disease is increased in vivo by the presenilin 1 and 2 and APP mutations linked to familial Alzheimer's disease. *Nat. Med.* **2,** 864–870.

Sherrington R., Rogaev E. I., Liang Y., Rogaeva E. A., Levesque G., Ikeda M., Chi H., Lin C., Li G., Holman K., Tsuda T., Mar L., Foncin J.-F., Bruni A. C., Montesi M. P., Sorbi S., Rainero I., Pinessi L., Nee L., Chumakov I., Pollen D., Brookes A., Sanseau P., Polinsky R. J., Wasco W., DaSilva H. A. R., Haines J. L., Pericak-Vance M. A., Tanzi R. E., Roses A. D., Fraser P. E., Rommens J. M., and St. George-Hyslop P. H. (1995) Cloning of a gene bearing missense mutations in early-onset familial Alzheimer's disease. *Nature* **375,** 754–760.

Sumikawa K. and Miledi R. (1989) Change in desensitization of cat muscle acetylcholine receptor caused by coexpression of *Torpedo* actylcholine receptor subunits in *Xenopus* oocytes. *Proc. Natl. Acad. Sci. USA* **86,** 367–371.

Thinakaran G., Borchelt D. R., Lee M. K., Slunt H. H., Spitzer L., Kim G., Ratovitsky T., Davenport F., Nordstedt C., Seeger M., Hardy J., Levey A. I., Gandy S. E., Jenkins N. A., Copeland N. G., Price D. L., and Sisodia S. S. (1996) Endoproteolysis of presenilin 1 and accumulation of processed derivatives in vivo. *Neuron* **17,** 181–190.

Thinakaran G., Regard J. B., Bouton C. M. L., Harris C. L., Price D. L., Borchelt D. R., and Sisodia S. S. (1998) Stable association of presenilin derivatives and absence of presenilin interactions with APP. *Neurobiol. Dis.* **4,** 438–453.

Tigyi G., Dyer D., Matute C., and Miledi R. (1990) A serum factor that activates the phosphatidylinositol phosphate signaling system in *Xenopus* oocytes. *Proc. Natl. Acad. Sci. USA* **87,** 1521–1525.

Van Broeckhoven C. (1995) Presenilins and Alzheimer disease. *Nat. Genet.* **11,** 230–232.

Weber L., Leissring M. A., Yang A. T., Glabe C. J., Cribbs D. H., and LaFerla F. M. (1996) Presenilin-1 immunoreactivity is localized intracellulary in Alzheimer's disease brain, but not detected in amyloid plaques. *Exp. Neurol.* **143,** 37–44.

Yao Y., Choi J., and Parker I. (1995) Quantal puffs of intracellular Ca^{2+} evoked by inositol trisphosphate in *Xenopus* oocytes. *J. Physiol. (Lond.)* **482,** 533–553.

Zhang J., Kang D. E., Xia W., Okochi M., Mori H., Selkoe D. J., and Koo E. H. (1998) Subcellular distribution and turnover of presenilins in transfected cells. *J. Biol. Chem.* **273,** 12436–12442.